Theoretical Population Biology 123 (2018) 9–17

Contents lists available at ScienceDirect

Theoretical Population Biology

journal homepage: www.elsevier.com/locate/tpb

A downstream drift into chaos: Asymmetric dispersal in a classic density dependent population model

Laura S. Storch [a,*], James M. Pringle [b]

[a] Department of Mathematics, 200 Ukrop Way, College of William and Mary, Williamsburg, VA 23185, USA
[b] Department of Earth Sciences and the Institute for Earth, Ocean, and Space, 39 College Rd., University of New Hampshire, Durham, NH 03824, USA

ARTICLE INFO

Article history:
Received 28 August 2017
Available online 3 May 2018

Keywords:
Asymmetric dispersal
Spatial population model
Chaotic dynamics
Logistic map
Gaussian kernel dispersal
Sustainable management

ABSTRACT

In the ocean, propagules with a planktonic stage are typically dispersed some distance downstream of the parent generation, introducing an asymmetry to the dispersal. Ocean-dwelling species have also been shown to exhibit chaotic population dynamics. Therefore, we must better understand chaotic population dynamics under the influence of asymmetrical dispersal. Here, we examine a density-dependent population in a current, where the current has both a mean and stochastic component. In our finite domain, the current moves offspring in the downstream direction. This system displays a rich variety of dynamics from chaotic to steady-state, depending on the mean distance the offspring are moved downstream, the diffusive spread of the offspring, and the domain size. We find that asymmetric dispersal can act as a stabilizing or destabilizing mechanism, depending on the size of the mean dispersal distance relative to the other system parameters. As the strength of the current increases, the system can experience period-halving bifurcation cascades. Thus, we show that stability of chaotic aquatic populations is directly tied to the strength of the ocean current in their environment, and our model predicts increased prevalence of chaos with decreasing dispersal distance. Climate change is likely to alter the dispersal patterns of many species, and so our results have implications for conservation and management of said species. We discuss the management implications, particularly of exploited species.

1. Introduction

Populations in rivers, streams, and oceans are primarily dispersed by currents with a dominant preferred direction. Aquatic species have been shown to exhibit chaotic population dynamics (Hsieh et al., 2006; Glaser et al., 2014). Therefore, we must work to better our understanding of chaotic populations in asymmetrical dispersal environments. This is particularly true for vulnerable populations, such as exploited fish and shellfish species, that we struggle to manage sustainably (Mullon et al., 2005). It is also critical that we understand the reaction of chaotic populations to environmental changes, given our rapidly changing climate. These changes are likely to increase the number of populations classified as "vulnerable" and create new management challenges (McLaughlin et al., 2002). Here, we examine the interplay between chaos and asymmetric dispersal via a spatially explicit population in a current. The current has both mean and stochastic dispersal components. We illustrate that, depending on the relationships between mean dispersal distance, stochastic dispersal distance, and domain size, asymmetrical dispersal can serve as a destabilizing force or a stabilizing force in a population.

Chaotic growth paired with asymmetrical dispersal is prevalent in models of open flow systems, which apply to fluid dynamics, atmospheric models, and other physical systems (e.g., Lind et al., 2002; Jiang and Parmananda, 1998; Willeboordse and Kaneko, 1994, 1995). While a subset of the open flow literature claims to have generic applicability to physical and biological systems (Willeboordse and Kaneko, 1994, 1995), these models cannot realistically be used to inform ecologists about chaotic populations in asymmetrical dispersal environments. For example, implicit parameters exist within some of the models, and/or constraints on parameters limit applicability to a very narrow range of scenarios that could occur in an ecological system. We have built our model to avoid these limiting factors, and will thus fill a gap in the ecological literature pertaining to chaotic populations in unidirectional flows.

Extensive analysis has been performed on symmetrically dispersing chaotic populations, i.e., diffusive-type dispersal (Ruxton and Doebeli, 1996; Doebeli and Ruxton, 1998; Saravia et al., 2000; Labra et al., 2003; Storch et al., 2017). This type of dispersal is an appropriate approximation for species making small random movements over a terrain (e.g., insects) or immobile species transported via an external forcing with no preferred directionality,

* Corresponding author.
E-mail addresses: lstorch@wm.edu (L.S. Storch), jpringle@unh.edu (J.M. Pringle).

https://doi.org/10.1016/j.tpb.2018.04.003
0040-5809/

such as animals ingesting and dispersing seeds (Skellam, 1951; Okubo, 1980). The symmetric dispersal mechanism can be represented by a dispersal kernel or discretized diffusion. A large body of research employing the latter takes the form of 1- or 2-dimensional coupled map lattices (Kaneko, 1984, 1989, 1992; Solé et al., 1992; Willeboordse, 2002, 2003; White and White, 2005) with a logistic map (May, 1976) growth mechanism.

The logistic map is a classic, zero-dimensional, density-dependent, population model with chaotic dynamics for high enough growth rates. The logistic map is:

$$p_{n+1} = ap_n(1 - p_n)$$

where n is the time index, p is the nondimensionalized population (nondimensionalized by the carrying capacity), and a is the growth parameter. The logistic map is a discrete-time analog of the continuous-time logistic equation (Verhulst, 1845). The discrete time logistic map has fundamentally different dynamics from the continuous time logistic equation, and for some species, discrete, non-overlapping generations are a more accurate model for the population behavior (e.g., some anadromous fish, many benthic organisms).

As a approaches 3.57 the dynamics evolve from steady state through a bifurcation cascade, and for $a > 3.57$, the logistic map displays predominantly chaotic behavior. There are small pockets of periodic behavior for select values of a above 3.57, and the population goes extinct for $a > 4$. For $p > 1$ the population diverges and loses physical meaning.

When chaotic growth is combined with diffusive-type (symmetric) dispersal along a spatial domain, a variety of spatio-temporal behaviors are observed, depending on the parameter combination. These behaviors range from periodic, to quasi-periodic, to spatio-temporal chaos (Kaneko, 1992). If we compare the characteristics of the classic logistic map (May, 1976) to these 1- and 2-dimensional coupled map lattices, there is a pronounced decrease in prevalence of chaotic behavior for the lattices over the same range of growth parameter, as the symmetrical dispersal serves to dampen or eliminate chaotic dynamics over both space and time.

This paper extends these results by adding a dominant current to the system. Our model uses a modified logistic map as the growth mechanism, and pairs this with a biased Gaussian dispersal kernel. Propagules (offspring) are moved some mean distance downstream of the parent generation, while also diffusing randomly about the mean. Since currents in real physical systems have variation, e.g., ocean eddies, the random diffusive component is a reasonable addition to the mean dispersal, as we would not reasonably expect that propagules originating from a specified discrete upstream location would all disperse to the same location downstream.

We prefer Gaussian kernels over discretized diffusion for several reasons. In a Gaussian kernel, the length scales of the diffusive dispersal distance and mean dispersal distance are not linked to the discrete spacing of the model domain. Therefore, the diffusive dispersal distance or mean dispersal distance can easily be altered to suit a variety of population dispersal scenarios without altering the underlying chosen spatial discretization. The spatial discretization length scale and the mean and diffusive dispersal length scales are not linked because the Gaussian kernel is not a discretized approximation of an inherently continuous system, as discretized diffusion is. Additionally, Gaussian kernels (and other shaped kernels) have a long history in the ecological literature because they make reasonable approximations of real dispersal (Chesson and Lee, 2005).

Similar unidirectional flow models exist in the coupled map lattice literature, and while they are not particularly ecologically applicable, they are dynamically rich and we can use knowledge of their dynamics to inform the analysis of our ecologically applicable model. One such model example is studied by Willeboordse and Kaneko (1994, 1995) and takes the form:

$$p_{n+1,i} = (1 - \epsilon)f(p_{n,i}) + \epsilon f(p_{n,i-1})$$

where i is a spatial index, n is a time index, p is the population abundance, $f(p)$ is the function $f(p) = 1 - ap^2$, and a is the growth parameter, as usual. In this model, ϵ dictates how asymmetrical the dispersal is, i.e., what portion of the population at location i originated from the adjacent upstream location $(i-1)$. This is the "one-way coupled logistic lattice" (OCLL). Essentially, it is an upwind discretization of the advection term of a fluid transport equation. The model exhibits parameter-driven bifurcation cascades, spatial bifurcations, and spatial chaos paired with temporal periodicity.

The OCLL has several features that make it difficult to apply to real-world systems. First, the population at any given location is only capable of moving one discrete location to the right (downstream) in one iteration. This directly ties the spatial scale of the mean dispersal distance to the spatial scale of the domain discretization since ϵ must be less than one, e.g., propagules can only move one grid cell downstream per generation. If we want to assume longer dispersal distances, we must also assume correspondingly poorer spatial resolution. Next, because this is a discretization of a continuous system (discretization of advection, upwind scheme, $\partial p/\partial t = -c(\partial p/\partial x)$), the nature of the discretization gives the model implicit diffusion, i.e., neighboring discrete patches interact in both upstream and downstream directions even though this is not apparent from the equation. The implicit diffusion term originates from the discarded higher order terms of the discretized derivative approximations, and is always equal to $\epsilon/2$ (for a derivation of this result please see Mesinger and Arakawa (1976), page 30). Implicit model parameters are not desirable attributes in an ecological model, as the aim is to understand population dynamics and how they are affected by changes in ecologically relevant parameters. Also, since the implicit diffusive term must always be equal to 1/2 the mean current strength, this essentially eliminates the direct applicability of this model to most systems. With the use of a Gaussian kernel, our model has separate advective (mean) and diffusive (stochastic) dispersal length scales, both of which are decoupled from the spatial discretization of the domain, and the diffusive dispersal is explicitly discrete. This allows us to explore a much wider range of dynamics and to apply our model to any ecological system with asymmetric dispersal.

Although improved understanding of chaotic populations in unidirectional flows is important for ensuring the future of our rapidly changing aquatic ecosystems, this problem is not addressed in an ecologically applicable way in the existing literature. Therefore, further work such as that presented here, must address this. We wish for our model to help fill this gap by incorporating explicit length scales of mean and stochastic dispersal terms, removing the unrealistic parameter constraints of the OCLL model, and testing an ecologically plausible parameter range. In this way, we introduce ecological features while still maintaining simplicity and applicability to a wide range of population scenarios. A complex interplay exists between chaotic density-dependent growth, mean dispersal distance, and stochastic diffusive dispersal distance, and we explore the range of dynamics that occur within this system, and show how populations react to changes in parameters. We will show that introducing a small amount of asymmetry to a previously symmetrical system can destabilize a population and induce chaotic behavior in a previously well-behaved population. Conversely, we will show that when the mean dispersal distance is approximately equal to the diffusive dispersal distance, populations have steady-state solutions, regardless of their behavior when the advection is weaker. Improving our understanding of the complex relationships between these parameters will in turn improve our understanding of population dynamics in asymmetric

dispersal environments, which will aid in conservation and management efforts of vulnerable populations.

2. Methods

We apply logistic growth and Gaussian kernel dispersal to a one-dimensional domain in a two-step process. The population in this model has no age structure, there are only adults and offspring (the propagules/larvae). First, propagules/larvae are grown at each discrete location in the domain. Then, the propagules are dispersed and settle as adults. In this way we model species with a mobile larval offspring stage and a sessile adult stage.

We modify the zero-dimensional (zero spatial dimension) logistic map such that it can be applied to discrete locations along a one-dimensional spatial domain. A one-dimensional domain is an appropriate approximation for, e.g., coasts, rivers, or riparian habitats. The propagule growth is dictated by:

$$l_{n+1,i} = ap_{n,i}(1 - \frac{p_{n,i}}{p_{loc}})$$

which is the "generalized logistic equation" from Li and Yorke (1975). Lowercase i is the spatial indexing and n is the time indexing. Lowercase l is the number of propagules/larvae in the $n+1$ generation, which depends on the growth parameter, a, and the population, p, from the previous n generation. p_{loc} is the carrying capacity of a local discrete patch, where

$$p_{loc} = \frac{p_{total}}{N}$$

N is the number of discrete patches in the domain and p_{total} is the carrying capacity for the summed population across the entire domain ($p_{total} = 1$). The dynamics of the model are qualitatively insensitive to changes in N, as long as it is sufficiently large to smoothly resolve the dispersal kernel.

The original logistic map allows the population to diverge away from physically meaningful values for $a > 4$, so we fix this by imposing biologically realistic constraints on the propagule vector, l. If a location in the propagule vector has a negative value, we assume that local resources were too limited to produce offspring in that location, and the larval production in that location is set to zero.

After the larval production, the propagules/larvae are dispersed away from their parents via a convolution between the vector of propagules and a normalized biased Gaussian dispersal kernel. The normalized biased Gaussian kernel is:

$$f_i = f(x_i) = \frac{1}{\sigma\sqrt{2\pi}} e^{\frac{-(x_i-\mu)^2}{2\sigma^2}}$$

where σ is the standard deviation, μ is the mean (location of the Gaussian center), and x_i is a discrete location in the spatial domain. $\sum_{i=-\infty}^{\infty} f(x_i) = 1$ and our domain is of finite length, so the sum of the Gaussian over the domain will be less than one. The mean dispersal distance per generation is μ, the mean distance a larva is dispersed downstream from a parent. The diffusive dispersal distance per generation is σ. The diffusive dispersal distance adds a stochastic element to the dispersal by spreading the propagules from a given upstream location across multiple downstream locations, at an average distance of μ. Fig. 1 provides an illustration of the dispersal for one generation of a population, where the offspring have been dispersed an average distance μ downstream of the parents with a diffusive spread σ.

The discrete convolution between the propagule vector, l, and the Gaussian kernel, f, is:

$$p_i = (f * l)_i = \sum_{j=1}^{N} f_{i-j} l_j$$

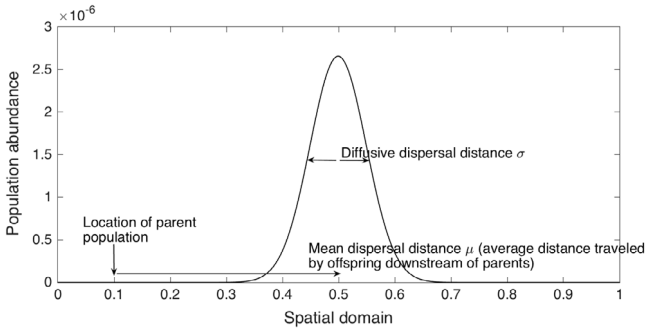

Fig. 1. Cartoon of offspring dispersing downstream of the parent population for one generation. The parent population was located at $x = 0.1$ on the x-axis, σ is 5% of the domain size, and μ is 40% of the domain size.

N is the total number of discrete patches in the domain ($N = 1001$), and i and j are location indices for those discrete spatial locations. The resulting population vector, p, is longer than the propagule vector and Gaussian kernel vector and therefore has individuals that disperse outside of the confines of the spatial domain. The population vector is symmetrically truncated on either side such that the length of p matches the length of l, and the individuals residing in these "out of bounds" sections of the population vector are considered lost to the system. This represents propagules dispersing outside of their habitable range and dying, and in this way we introduce absorbing boundary conditions. Because a species usually has a limited range of habitability depending on temperature, food availability, or other environmental factors, absorbing boundaries are the most biologically realistic.

Following Storch et al. (2017) we iterate for 10^4 generations, which is long enough to remove transients and to examine persistent chaotic behavior in the settled system. We acknowledge the long-lived nature of the transients in our system as dynamically interesting and ecologically relevant (Hastings and Higgins, 1994), but our model dynamics are rich and complex in the absence of transients, so we explore the dynamics of the fully-evolved system in this initial investigation. Again, following Storch et al. (2017), our parameter space explores $3.5 \leq a \leq 4$, $0.01 \leq \sigma/D \leq 0.20$, and $0 \leq \mu/\sigma \leq \sqrt{2\ln(a)}$, where D is the size of the domain. We choose this range of a because it exists mostly within the chaotic growth range of the classic logistic map (though our model is not limited to $a < 4$ because we remove the ability to produce negative propagules). For lower values of a, the dynamics of the model are periodic or steady state. For $\sigma/D > 0.20$ the dispersal is so large relative to the domain size that the spatial model begins to essentially collapse back to the zero-dimensional case as the diffusive dispersal completely homogenizes the domain (Storch et al., 2017). Because the population with large σ/D is completely uniform across the domain, it is analogous to a point-source population, and therefore, the dynamics can be understood by the already well-studied classic logistic map (May, 1976). Finally, we explore $0 \leq \mu/\sigma < \sqrt{2\ln(a)}$ because as μ/σ approaches $\sqrt{2\ln(a)}$, extinction occurs. The extinction criterion is derived in Byers and Pringle (2006).

The initial conditions of the model are random stochastic noise, where each discrete location is assigned a random population abundance between zero and 0.001, such that the total population summed across all locations is less than the carrying capacity of the domain, p_{total}. Fig. 2 shows an example initial condition for a population, the population after one iteration, and the population after 1000 iterations. The random initial condition is quickly smoothed out by the Gaussian kernel dispersal, but there is a period of transient dynamics before the system settles (the transience is not an artifact of the chosen initial condition).

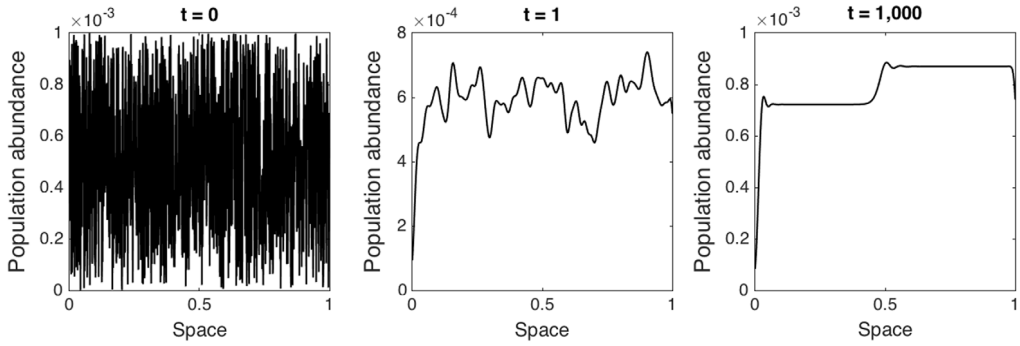

Fig. 2. Example of random initial conditions for a population ($t = 0$, first plot), the population distribution after one generation ($t = 1$, middle plot), and the population distribution after 1000 generations ($t = 1000$, last plot) for one example parameter combination. Parameters are $a = 3.60$, $\sigma = 0.01$, $\mu = 0.01$. This particular parameter combination settles to period-2 dynamics after an initial period of transience.

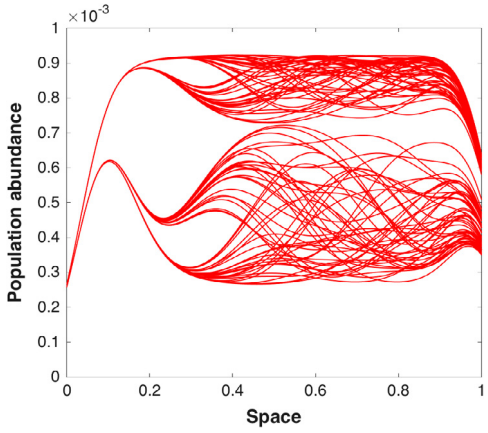

Fig. 3. Example population distribution for $a = 3.70$, $\Omega = 0.06$, $\Psi = 0.5$. The distribution pattern is created by overlapping 100 consecutive generations, which are recorded after an initial period of 10^4 generations. The relative mean dispersal strength is high enough to introduce an obvious asymmetry to the distribution pattern. The very beginning of the domain (upstream edge) has a steady state solution that becomes a period-2 solution slightly farther downstream, which becomes a period-4 solution even further downstream, before the spatial distribution patterns are non-overlapping and the dynamics become chaotic (the red color indicates that the dynamics of the summed total population are chaotic). (For interpretation of the references to color in this figure legend, the reader is referred to the web version of this article.)

In this study, we classify chaos by calculating the L2 norm of the divergence between a perturbed and unperturbed population:

$$div_n = \sqrt{\sum_{i=1}^{N} |p_{n,i} - per_{n,i}|^2}$$

where N is the total number of discrete patches, p is the unperturbed population, per is the perturbed population, n is the time indexing, and i is the spatial indexing. Two identical initial populations evolve over time for 10,000 generations to remove transient behavior. Then, an arbitrarily small, random perturbation (on order 10^{-10}) is applied once to each patch in one of the populations. Each population evolves for an additional 100 generations, and the norm of the divergence between the summed total populations over those 100 generations is calculated. In other words, the norm is calculated over all space for generations $n = 10{,}001$ to $n = 10{,}100$. If the divergence between the two populations is growing over time, the system is considered chaotic. In this way, we classify the dynamics of the total population, as opposed to the dynamics of each discrete location in the domain. Please refer to Storch et al. (2017) for a detailed justification of this choice over the full spectrum of Lyapunov exponents (Lyapunov, 1992).

3. Results

We characterize our system with the following parameters: a (the growth parameter), $\Psi = \mu/\sigma$ (the relative mean dispersal strength), and $\Omega = \sigma/D$ (the relative diffusive dispersal strength), where μ is the mean dispersal distance (mean of the Gaussian), σ is the diffusive dispersal distance (standard deviation of the Gaussian), and D is the size of the domain. We choose these parameters because the persistence criterion for a population in an asymmetrical dispersal environment directly depends on Ψ and a (Byers and Pringle, 2006), and because Ψ and Ω are both nondimensional and thus our results are applicable to any sized ecological system. The Buckingham π theorem of dimensional analysis states that a system can be fully represented by i nondimensional parameters, where i is equal to the number of original system parameters (n) minus the number of physical dimensions (k). For this model, the original system has $n = 4$ parameters (μ, σ, D, and a) with $k = 1$ physical dimensions (the one physical dimension is length, as a is already a dimensionless measure of growth) such that the reduced parameter set $i = n - k = 3$ (Buckingham, 1914). Therefore, we conclude that Ψ, Ω, and a can fully represent the system.

The system displays a variety of dynamics ranging from steady state to chaotic, but Fig. 3 provides an example of commonly observed population dynamics in this model. The population distribution pattern is made by overlapping 100 consecutive generations. The current is strong enough to induce an obvious asymmetry in the distribution of the population, where upstream (beginning of the domain), the 100 consecutive population distributions display steady state/periodic dynamics (repeating spatial distribution patterns), and downstream the population distributions are chaotic (non-repeating spatial distribution patterns). We will discuss this "spatial bifurcation" in detail in the following paragraphs.

In the model, we characterize a general pattern in the evolution of the dynamics, where for arbitrarily small Ψ (relative mean dispersal strength), asymmetrical dispersal serves to destabilize the system and chaos is prevalent. Population distributions that are spatiotemporally periodic for $\Psi = 0$ become quasi-periodic or spatiotemporally chaotic. As Ψ increases, the system experiences a "reverse", period-halving bifurcation and the dynamics evolve from chaotic, to high periodicity, to low periodicity, to steady state. We visualize this general pattern of evolution in Fig. 4. Fig. 4 illustrates the general behavioral dependence on a, Ψ, and Ω, but is not meant to serve as an illustration of mathematically rigorously defined boundaries. The left plot is applicable for parameter combinations that yield chaotic dynamics for arbitrarily small Ψ. This generally tends to apply to the middle and high range of $3.5 \leq a \leq 4$ paired with small to mid-range Ω. For parameter combinations that are never chaotic, there is a slow reduction of the periodicity until the population distribution achieves steady state.

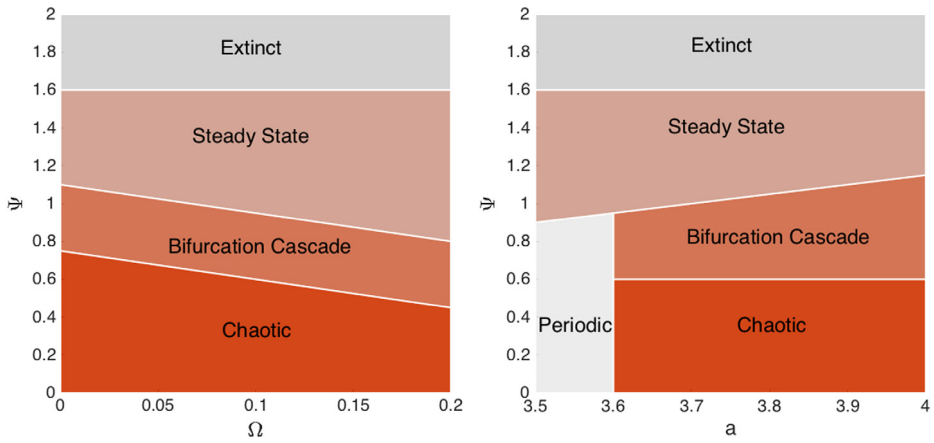

Fig. 4. General phase diagram of dynamical behavior dependent on relative mean dispersal strength $\Psi = \mu/\sigma$ and relative diffusive dispersal strength $\Omega = \sigma/D$ (left figure), and relative mean dispersal strength Ψ and growth parameter a (right figure). This general sketch is not meant to serve as an illustration of well-defined boundaries, as the boundary between dynamics in the left figure depend on a, and the boundary between dynamics in the right figure depend on Ω. Therefore, each figure illustrates, on average, where the various observed dynamical regimes are likely to occur. The left figure applies for population distributions that experience chaotic dynamics for arbitrarily small Ψ.

In Fig. 4, holding a or Ω constant and increasing the relative mean dispersal strength (Ψ) will yield the aforementioned dynamic evolution from chaotic to bifurcation cascade to steady state dynamics. We observe the same general evolution of behavior from chaotic to periodic with increasing relative diffusive dispersal strength (Ω), but over a limited range of Ψ (when large, the relative mean dispersal strength determines the dynamics of the system, and the system therefore has weaker dependence on change in Ω).

Fig. 5 is an example bifurcation diagram of the period-halving bifurcation cascade for $a = 3.8$, $\Omega = 0.1$, and $0 \leq \Psi \leq 1.5$. The bifurcation diagram is created by calculating the total population over 100 consecutive generations for each Ψ (after transients are removed). The total populations for 100 generations for each parameter combination are then plotted together. Vertical slices across total population values (the y-axis) for a given Ψ indicate different dynamical states. For example, vertical slices with a single population value indicate that the solution for that parameter combination is steady state, while vertical slices with many non-overlapping population values indicate that the solution for that parameter combination is chaotic. For this particular combination of a and Ω, the $\Psi = 0$ solution is periodic, but quickly transitions to chaos for small relative mean dispersal strength, Ψ. For $\Psi \approx 0.6$, the population begins the period-halving bifurcation cascade, and for $\Psi \approx 1$ the population reaches a steady state solution.

This bifurcation diagram has several pronounced pockets of periodic behavior before the final transition to periodic/steady-state dynamics. This is typical of the dynamical transitions in bifurcation cascades, and is analogous to the pockets of periodicity observed during the transition to chaos in the bifurcation diagram of the classic logistic map (Campbell, 1979). In the $\Psi = 0$ model, we witness frequent and abrupt switching between periodic and chaotic behavior with arbitrarily small changes in Ω or a (Storch et al., 2017), where zooming in on smaller ranges of Ω or a reveals the same pattern of frequent switching. For the parameters shown in Fig. 5, there are several pockets of periodicity, but the frequent switching between chaotic and periodic behavior is largely absent (we confirmed the absence of frequent dynamical switching by running the model again with smaller incremental increases in Ψ, for the same parameter range in Fig. 5).

For parameter combinations that are fully spatiotemporally chaotic in the $\Psi = 0$ model (Storch et al., 2017), the transition from chaotic to steady state dynamics with increasing Ψ may not occur through an easily identifiable period-halving bifurcation cascade. This is because the downstream area (right side of the domain) maintains chaotic dynamics over a long range of increasing Ψ values. The transition to periodic dynamics is then very abrupt and a bifurcation cascade cannot be resolved (illustrated in the supplemental material, figure 1S).

As the system experiences a parameter-driven period-halving bifurcation cascade for increasing Ψ, we witness corresponding spatial bifurcations across the domain. This phenomenon is well documented by Willeboordse and Kaneko (1994, 1995). In Fig. 6 we illustrate the spatial bifurcations for several example values of Ψ, holding a and Ω constant. The population distribution patterns are created by overlapping 100 consecutive iterations of the model. The beginning of the domain (upstream) consistently has a steady-state population, further downstream has a period-2 population, further downstream has a period-4 population, and so on, where the highest periodicity achieved is located near the downstream edge of the spatial domain, and corresponds to the parameter bifurcations occurring with change in Ψ. A movie of this phenomenon is available in the supplementary material (Movie 1S).

As the relative mean dispersal strength (Ψ) continues to grow, eventually Ψ is so strong that the entire population is swept downstream and goes extinct. The extinction criterion for populations in a current is derived by Byers and Pringle (2006) in a semi-infinite domain, and is a function of the growth parameter a, mean dispersal distance μ, and diffusive dispersal distance σ. In order for a population to persist in a domain with a unidirectional current, the following criterion must be satisfied:

$$\ln(a) > \frac{\mu^2}{2\sigma^2}$$

or equivalently,

$$\ln(a) > \frac{1}{2}\Psi^2.$$

We find that our model is in generally good agreement with the above criterion. Our model will increasingly deviate from the criterion as Ω increases because the semi-infinite domain assumption is violated. Fig. 7 illustrates the largest μ possible for a given σ that allows population persistence (the slope of the line is therefore Ψ).

4. Discussion

Our model displays a rich variety of dynamics depending on the growth parameter (a), relative diffusive dispersal strength

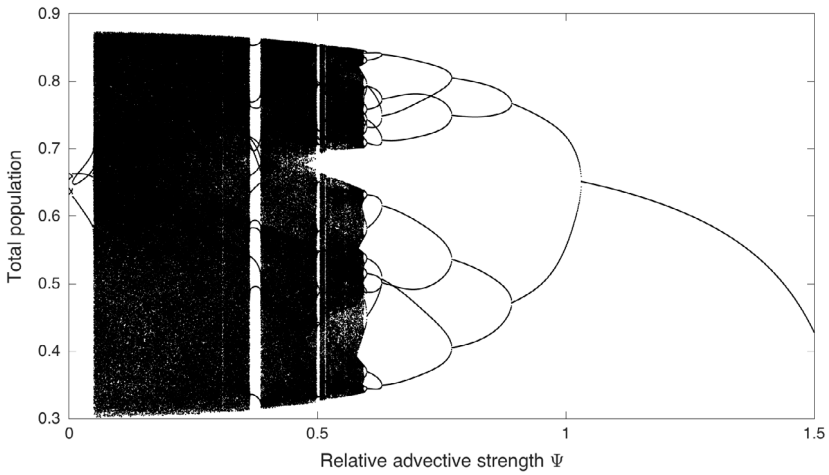

Fig. 5. Period-halving bifurcation cascade for $a = 3.80$, $\Omega = 0.10$, relative mean dispersal strength ($\Psi = \mu/\sigma$) increasing along the x-axis. The bifurcation diagram is created by recording the total population over 100 iterations for all of the Ψ between 0 and 1.50. Each vertical slice contains all of the total population values over 100 iterations for one parameter combination of a, Ω, Ψ. Therefore, if there is a smear of values, it indicates that the population dynamics are chaotic (nonrepeating values for total population). This period-halving bifurcation diagram has several pronounced pockets of periodicity between $0 \leq \Psi \leq 0.6$.

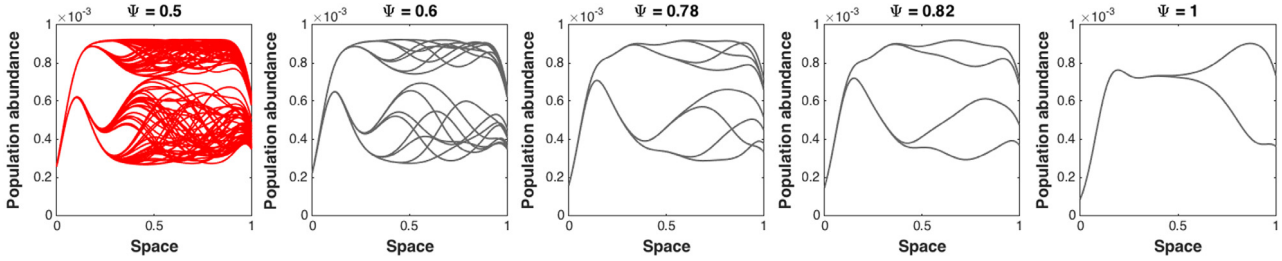

Fig. 6. Spatial bifurcations corresponding to the period-halving bifurcation cascade with increasing relative mean dispersal strength, Ψ ($a = 3.70$ and $\Omega = 0.06$, both held constant). Red color indicates chaotic behavior and gray indicates periodic behavior. The population distribution patterns are created by overlapping 100 consecutive iterations of the model. The first plot is for the smallest Ψ and displays chaotic behavior. As Ψ increases in each graph, the population distribution goes through a spatial bifurcation, which are pictured in gray for period 16, period 8, period 4, and period 2 (moving left to right). (For interpretation of the references to color in this figure legend, the reader is referred to the web version of this article.)

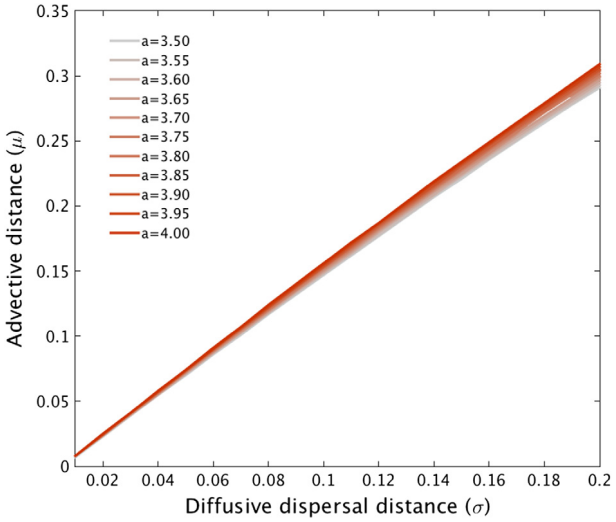

Fig. 7. Largest mean dispersal distance (μ) for a given diffusive dispersal distance (σ) that allows the population to persist. There are 11 curves plotted for the 11 growth parameter (a) values tested. The slope of the curves is nearly linear and approximately $\Psi \approx 1.5$. The curves have similar slopes because our selected range of $3.5 \leq a \leq 4$ have nearly identical persistence criterion. The curves separate more at the high end of σ because each parameter combination was tested for extinction under the same time frame, but populations with high σ take longer to go extinct. Therefore, if the larger σ values were allowed to evolve over a correspondingly larger time frame, the curves would be closer together as they are at the low end of σ.

(Ω), and relative mean dispersal strength (Ψ). When Ψ is small, asymmetrical dispersal is a destabilizing force and chaotic behavior is prevalent across the tested parameter space of a and Ω. As the relative mean dispersal strength increases, population distributions experience a period-halving bifurcation cascade with corresponding spatial bifurcations until they reach steady state solutions.

Because our parameters are nondimensionalized, we can explain the dynamics of our model in terms of changing the effective domain size or changing the relative size of the upstream region. Here, the "upstream region" is defined as the region closest to the beginning of the domain, which displays periodic behavior even if the population is chaotic downstream, as in Fig. 3.

In Fig. 6, as Ψ increases through the period-halving bifurcation cascade (with corresponding spatial bifurcations), the size of the upstream region is effectively increasing with respect to the domain size. Therefore, moving through the images from left to right in Fig. 6 is equivalent to observing increasingly smaller sections of the upstream region from the leftmost (red) image. For example, in the leftmost (red) image, the region between $x = 0$ and $x \approx 0.2$ has a period-4 cycle, the region between $x = 0$ and $x \approx 0.1$ has a period-2 cycle, and so forth. The more we "zoom in" on the upstream region, the less of the complicated downstream dynamics we observe. So, each time we increase Ψ, we effectively increase the extent of the upstream region (or decrease domain size).

We visualize a similar dynamical evolution for increasing the relative diffusive dispersal strength ($\Omega = \sigma/D$) in Fig. 8. With

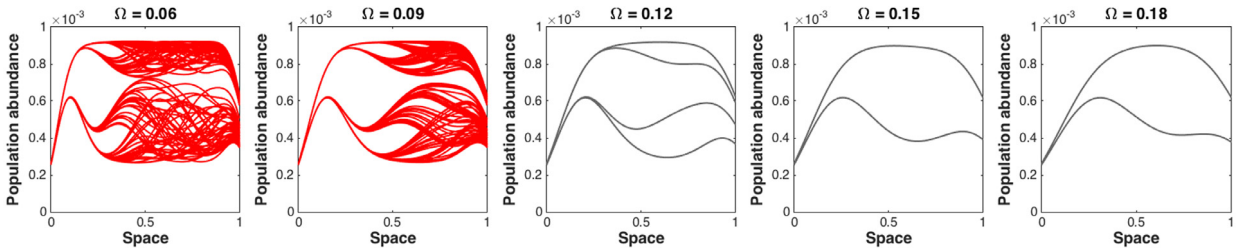

Fig. 8. Evolution of behavior for $a = 3.70$, $\Psi = 0.5$, relative diffusive strength (Ω) increasing. Red graphs indicate chaotic behavior. The patterns are created by overlapping 100 consecutive population distributions. As Ω increases from left to right, the domain size is effectively shrinking and the chaotic dynamics are removed from the system. (For interpretation of the references to color in this figure legend, the reader is referred to the web version of this article.)

increasing Ω, the domain size is effectively shrinking, and with each successive decrease, we move more complicated dynamics outside of the confines of the domain. In this way, we move from chaotic dynamics on the left graph to period-2 dynamics on the right graph.

Period-halving bifurcations are well-documented in the immigration literature (e.g., McCallum, 1992; Stone, 1993; Rohani and Miramontes, 1995; Stone and Hart, 1999). In these models, a constant immigration term is added to the iterative map that dictates population growth. For example, a logistic map with added immigration takes the form:

$$p_{n+1} = ap_n(1 - p_n) + I$$

where I is a constant number of migrants added to the population in each generation. Depending on the iterative map used, this immigration term can cause period-halving bifurcation cascades with increasing growth parameter, a. Period-halving is observed in unimodal maps with a "tail" or plateau, such as the Ricker map (Ricker, 1954), and cannot occur in the zero-spatial dimension logistic map due to the strictly concave-down shape of the p_{n+1} versus p_n curve (Stone and Hart, 1999). We, however, observe period-halving in a spatially extended system with logistic map growth. The downstream region receives upstream "immigrants" in each generation, although this number is not constant. However, we may still provide the cautionary statement that spatially extended systems are unlikely to be governed by the same rules as their spatially unresolved counterparts. A mathematically rigorous analysis of the mechanism leading to period-halving in the spatially extended logistic map is beyond the scope of this paper, but warranted.

The spatial bifurcations observed in this system are a result of advection in a finite domain. Although the upstream region of the domain displays more stable dynamics than the downstream region, the upstream edge is not less susceptible to chaotic behavior, the behavior is simply moved downstream (and in fact, the upstream edge has higher effective growth, which would imply increased likelihood of chaos). We illustrate this, in detail, in an upcoming publication, by applying localized perturbations to different regions in the domain. Perturbations applied to the upstream region grow and propagate downstream, and can induce chaotic dynamics where they were previously absent. Thus, the upstream edge is sensitive to perturbation, but the resulting complicated dynamics move downstream (Storch and Pringle, unpublished).

In the symmetrical dispersal scenario ($\Psi = 0$ system), there is frequent switching between differing dynamical behaviors (e.g., periodic vs chaotic) as parameters change (Storch et al., 2017). Such frequently switching dynamics has implications for predicting the behavior of these systems and for managing them appropriately. In the asymmetrical dispersal scenario, this rapid switching between dynamics is largely destroyed, although regions of rapid switching can still exist, particularly as Ψ enters into and transitions through the period-halving bifurcation cascade. Therefore, we might expect more smoothly transitioning dynamics in the asymmetrical dispersal model with changes in parameters, but we must still be aware of the potential for rapid dynamical changes, and understand that rapid dynamical changes can be driven by the underlying system dynamics and are not stochastic in nature.

4.1. Real-world applications and management applications

There are many real-world scenarios that would affect the parameters of our modeled system, and would consequently have significant impacts on its dynamics. For example, in our model, in each generation propagules are dispersed a mean distance μ downstream, so if a species spends a longer amount of time in the larval (propagule) stage, they spend a longer amount of time drifting in the current, and the effective dispersal distance of that species is therefore longer. The time a species spends in the larval stage (planktonic larval duration, T_{PLD}) would also change the relative mean dispersal strength of the system ($\Psi = \mu/\sigma$), as the mean dispersal distance is proportional to T_{PLD} but the diffusive dispersal distance is proportional to $T_{PLD}^{1/2}$ ($\mu \propto T_{PLD}$ and $\sigma \propto \sqrt{T_{PLD}}$, Siegel et al., 2003).

The time a species spends in the larval stage is dependent on the temperature of the species' habitat (Hoegh-Guldberg and Pearse, 1995), and so the dispersal distance of propagules is dependent on the temperature of the species domain. For example, O'Connor et al. (2007) approximates the relationship between T_{PLD}, dispersal, and temperature, by aggregating dozens of data sets across multiple species. This relationship predicts, e.g., for an increase in temperature from 10 °C to 12 °C, T_{PLD} will decrease from ≈40 days to ≈32 day, which in turn decreases the dispersal distance from ≈140 to ≈110 km, a 20% reduction in dispersal distance (for typical alongshore currents). Our changing global climate has already brought about a rise in ocean temperatures (Hansen et al., 2006), and so our model predicts possibly dramatic changes in the population dynamics of a species with a change in temperature.

Lastly, the strength of the current itself varies seasonally/yearly, and so the dispersal distance of a species will also depend on which season they spawn (Byers and Pringle, 2006). We have illustrated how temperature and current strength influence the dispersal of propagules, but there are many physical factors that directly affect larval dispersal distance and development, most of which will be altered by climate change (e.g., ocean acidification, Riebesell et al., 2000).

Thus, we can conclude there is significant potential for the dynamics of some species to be dramatically altered by climate change, and management should anticipate and prepare for these potentially dramatic changes. Changes in larval dispersal will not simply affect the mean dispersal distance, but also the dynamics of a species, potentially shifting species from periodic to

chaotic regimes or vice-versa (rising temperatures suggests shortened dispersal distances, which suggests increased prevalence of chaos). Prediction of critical dynamical transitions is a difficult task and a current area of active research (Scheffer et al., 2009), but managers and policy makers can employ conservative prevention/remediation methods without the direct ability to predict said changes.

Presence of chaotic dynamics in marine species has been well established in the literature, both as an innate feature of complex marine systems (e.g., Klein et al., 2016), and one that can be exacerbated by exploitation (e.g., Anderson et al., 2008; Glaser et al., 2014). As we anticipate potentially dramatic changes in population dynamics due to various external factors, with the possibility of increased prevalence of chaos, we suggest, at minimum, more conservative catch limits on exploited species in the interest of lowering extinction risk as population volatility increases. For example, an increase in population variance could lead to a proportional reduction in allowable catch. In general, management of exploited species tends to assume higher levels of stability and linearity than exist in nature (e.g., Storch et al., 2017a), which may have disastrous effects as the dynamics of many species become less predictable and more volatile.

One potential application of this research could be to the design of Marine Protected Areas (MPAs). MPAs are designed to protect critical species habitats such as spawning grounds, which maximizes recruitment, while minimizing disruption to human exploitation efforts. Determining the optimal size and location(s) of MPAs is presently debated and differs by location, but the design of MPAs generally relies heavily on species dispersal patterns (Fogarty and Botsford, 2007), particularly the larval dispersal stage (Botsford et al., 2001). The results of our work can add to this larger discussion. Our results indicate that smaller domains are less likely to have chaotic dynamics (e.g., Figs. 6 and 8), and that changes in dispersal distance has the potential to dramatically alter species dynamics. Both results have implications for MPA design, especially under climate change.

With respect to the first result, we conclude that smaller MPAs may have reduced prevalence of chaotic dynamics. Although this may seem a desirable result, the model informs us that in a smaller domain, more larvae are being lost out of the system (or out of the confines of the MPA), and that more complicated dynamics are likely to be hiding further downstream. Thus, the increased regularity of the dynamics inside the MPA will come at the cost of higher prevalence of chaotic dynamics outside of the MPA, and with less potential protection of larvae. This combination would likely reduce efficacy of the MPA.

With respect to the second result, if a network of MPAs is in place for a particular species, and that species then transitions from, e.g., a periodic to a chaotic regime, the network of MPAs designed to manage and conserve the species may be rendered less effective, even if they are still protecting the correct locations with respect to spawning or other critical areas. Outside of the protected areas, the introduction of chaotic dynamics has implications for sustainable fishing practices (as mentioned above), and so decisions made outside of the protected area may have a disproportionate impact on the population as a whole. Destabilization of population dynamics and the potential for overharvesting also effects, by extension, the larger marine ecosystem, as species-to-species interactions and biodiversity may play important roles in ecosystem stability (Worm et al., 2006).

In general, understanding complex ocean ecosystems will continue to present challenges for ecologists, particularly as the dynamics of these systems become more volatile in the face of increasing human pressures and climate change. It is imperative that we use the many tools at our disposal, such as chaotic systems theory, to understand these systems if we wish to preserve them.

4.2. Future research

Avenues of future exploration for this work are many; we list several examples here.

The transients in the system have, to this point, been neglected. Because they are so long-lived, their ecological relevance cannot be ignored, and future work exploring the transient states of the system would yield insightful results.

Our spatially extended logistic map model experiences period-halving bifurcation cascades, which is not observed in the zero-spatial-dimensional logistic map. We believe this phenomenon warrants further investigation, along with a comparison to a spatially extended Ricker map system.

Our current model involves a population in which offspring disperse, settle, reproduce, and die. To expand to a wider variety of organisms, the model could include age structure and non-sessile adults, which would make the work far more applicable to fisheries, one of the most overexploited systems.

Lastly, this paper neglects the effects of perturbation, which no real-world system is free of. In upcoming work, we examine the effects of perturbation on the system (Storch and Pringle, unpublished)

Acknowledgments

The authors would like to thank MJ Fogarty, DO Jones, ES Klein, and an anonymous referee for thoughtful discussion of this research and the manuscript. This paper is comprised of content from a thesis submitted to the Graduate School at the University of New Hampshire as part of the requirements for completion of a doctoral degree. Funding for the research was provided by the US National Science Foundation (NSF) award OCE 0961344.

Conflict of interest

The authors declare that they have no conflict of interest.

Appendix A. Supplementary data

Supplementary material related to this article can be found online at https://doi.org/10.1016/j.tpb.2018.04.003.

References

Anderson, C.N.K., Hsieh, C., Sandin, S.A., Hewitt, R., Hollowed, A., Beddington, J., et al., 2008. Why fishing magnifies fluctuations in fish abundance. Nature 452, 835–839.

Botsford, L.W., Hastings, A., Gaines, S.W., 2001. Dependence of sustainability on the configuration of marine reserverse and larval dispersal distance. Ecol. Lett. 4, 144–150.

Buckingham, E., 1914. On physically similar systems; illustrations of the use of dimensional equations. Phys. Rev. 4, 345–376.

Byers, J.E., Pringle, J.M., 2006. Going against the flow: retention, range limits and invasions in advective environments. Mar. Ecol. Prog. Ser. 313, 27–41.

Campbell, D., 1979. An introduction to nonlinear dynamics. In: Stein, D.L. (Ed.), Lectures in the Sciences of Complexity. Addison-Wesley, Reading, MA.

Chesson, P., Lee, C.T., 2005. Families of discrete kernels for modeling dispersal. Theor. Popul. Biol. 67, 241–256.

Doebeli, M., Ruxton, G.D., 1998. Stabilization through spatial pattern formation in metapopulations with long-range dispersal. Proc. R. Soc. Lond. [Biol.] 265 (1403), 1325–1332.

Fogarty, M.J., Botsford, L.W., 2007. Population connectivity and spatial management of marine fisheries. Oceanography 20 (3), 112–123.

Glaser, S.M., Fogarty, M.J., Liu, H., et al., 2014. Complex dynamics may limit prediction in marine fisheries. Fish. Fish. 15 (4), 616–633.

Hansen, J., Sato, M., Ruedy, R., et al., 2006. Global temperature change. Proc. Natl. Acad. Sci. 103 (39), 14288–14293.

Hastings, A., Higgins, K., 1994. Persistence of transients in spatially structured ecological models. Science 263 (5150), 1133–1136.

Hoegh-Guldberg, O., Pearse, J.S., 1995. Temperature, food availability, and the development of marine interebrate larvae. Am. Zool. 35 (4), 415–425.

Hsieh, C., Reiss, C.S., Hunter, J.R., Beddington, J.R., May, R.M., Sugihara, G., 2006. Fishing elevates variability in abundance of exploited species. Nature 443 (7133), 859–862.
Jiang, Y., Parmananda, P., 1998. Spatial coherence in an open flow model. Phys. Rev. E 57 (3), R2499–R2502.
Kaneko, K., 1984. Period-doubling of kink-antikink patterns, quasiperiodicity in antiferro-like structures and spatial intermittency in coupled logistic lattice. towards a prelude of a "field theory of chaos". Progr. Theoret. Phys. 72 (3), 480–486.
Kaneko, K., 1989. Spatiotemporal chaos in one- and two-dimensional coupled map lattices. Physica D 37 (1–3), 60–82.
Kaneko, K., 1992. Overview of coupled map lattices. Chaos 2 (3), 279–282.
Klein, E.S., Glaser, S.M., Jordaan, A., Kaufman, L., Rosenberg, A.A., 2016. A complex past: historical and contemporary fisheries demonstrate nonlinear dynamics and a loss of determinism. Mar. Ecol. Prog. Ser. 557, 237–246.
Labra, F.A., Lagos, N.A., Marquet, P.A., 2003. Dispersal and transiet dynamics in metapopulations. Ecol. Lett. 6, 197–204.
Li, T.-Y., Yorke, J.A., 1975. Period three implies chaos. Am. Math. Monthly 82 (10), 985–992.
Lind, P.G., Corte-Real, J., Gallas, JAC., 2002. Modeling velocity in gradient flows with coupled-map lattices with advection. Phys. Rev. E 66, 016219.
Lyapunov, A.M., 1992. General Problem of the Stability of Motion. CRC Press, London; Washington, DC.
May, R.M., 1976. Simple mathematical models with very complicated dynamics. Nature 261 (5560), 459–467.
McCallum, H.I., 1992. Effects of immigration on chaotic population dynamics. J. Theoret. Biol. 154, 277–284.
McLaughlin, J.F., Hellmann, J.J., Boggs, C.L., Ehrlich, P.R., 2002. Climate change hastens population extinctions. Proc. Natl. Acad. Sci. 99 (9), 6070–6074.
Mesinger, F., Arakawa, A., 1976. Numerical Methods Used in Atmospheric Models, Vol. 1. International Council of Scientific Unions –World Meteorological Organization, Geneva.
Mullon, C., Freon, P., Cury, P., 2005. The dynamics of collapse in world fisheries. Fish. Fish. 6, 111–120.
O'Connor, M.I., Bruno, J.F., Gaines, S.D., Halpern, B.S., Lester, S.E., Kinlan, B.P., 2007. Temperature control of larval dispersal and the implications for marine ecology, evolution, and conservation. Proc. Natl. Acad. Sci. 104 (4), 1266–1271.
Okubo, A., 1980. Diffusion and Ecological Problems: Mathematical Models. Springer-Verlag.
Ricker, W.E., 1954. Stock and recruitment. J. Fish. Res. Board Can. 11 (5), 559–623.
Riebesell, U., Zondervan, I., Rost, B., et al., 2000. Reduced calcification of marine plankton in response to increased atmospheric CO2. Nature 407, 364–367.
Rohani, P., Miramontes, O., 1995. Immigration and the persistence of chaos in population models. J. Theoret. Biol. 175, 203–206.
Ruxton, G.D., Doebeli, M., 1996. Spatial self-organization and persistence of transients in a metapopulation model. Proc. R. Soc. Lond. [Biol.] 263 (1374). 1153–1158.
Saravia, L.A., Ruxton, G.D., Coviella, C.E., 2000. The importance of transients' dynamics in spatially extended populations. Proc. R. Soc. Lond. [Biol.] 267 (1454), 1781–1785.
Scheffer, M., Bascompte, J., Brock, W.A., Brovkin, B., Carpenter, S.R., Dakos, V., et al., 2009. Early-warning signals for critical transitions. Nature 461, 53–59.
Siegel, D.A., Kinlan, B.P., Gaylord, B., Gaines, S.D., 2003. Lagrangian descriptions of marine larval dispersion. Mar. Ecol. Prog. Ser. 260, 83–96.
Skellam, J.G., 1951. Random dispersal in theoretical populations. Biometrika 38 (1–2), 196–218.
Solé, R.V., Bascompte, J., Valls, J., 1992. Nonequilibrium dynamics in lattice ecosystems: Chaotic stability and dissipative structures. Chaos 2 (3), 387–395.
Stone, L., 1993. Period-doubling reversals and chaos in simple ecological models. Nature 365, 617–620.
Stone, L., Hart, D., 1999. Effects of immigration on the dynamics of simple population models. Theor. Popul. Biol. 55, 227–234.
Storch, L.S., Glaser, S.M., Ye, H., Rosenberg, A.A., 2017a. Stock assessment and end-to-end ecosystem models alter dynamics of fisheries data. PLoS One 12 (2), e0171644.
Storch, L.S., Pringle, J.M., Alexander, K.E., Jones, D.O., 2017b. Revisiting the logistic map: A closer look at the dynamics of a classic chaotic population model with ecologically realistic spatial structure and dispersal. Theor. Popul. Biol. 114, 10–18.
Storch, L.S., Pringle J.M., 2018. Perturbations grow downstream: The sometimes-chaotic response to disturbance of an asymmetrically dispersed population. Unpublished manuscript.
Verhulst, P., 1845. Recherches mathématiques sur la loi d'accroissement de la population. Nouv. Mém. Acad. R. Sci. Belles-Lett. Bruxelles 18, 1–41.
White, S.M., White, K.A.J., 2005. Relating coupled map lattices to integro-difference equations: dispersal-driven instabilities in coupled map lattices. J. Theor. Biol. 235, 463–475.
Willeboordse, F.H., 2002. Hints for universality in coupled map lattices. Phys. Rev. E 65 (2), 026202.
Willeboordse, F.H., 2003. The spatial logistic map as a simple prototype for spatiotemporal chaos. Chaos 13 (2), 533–540.
Willeboordse, F.H., Kaneko, K., 1994. Bifurcations and spatial chaos in an open flow model. Phys. Rev. Lett. 73 (4), 533–536.
Willeboordse, F.H., Kaneko, K., 1995. Pattern dynamics of a coupled map lattice for open flow. Physica D 86, 428–455.
Worm, B., Barbier, E.B., Beaumont, N., Duffy, J.E., Folke, C., Halpern, B.S., et al., 2006. Impacts of biodiversity on ocean ecosystem services. Science 314, 787–790.